Does Ekman Friction Suppress Baroclinic Instability?

SHIAN-JIANN LIN

Geophysical Fluid Dynamics Program, Princeton University, Princeton, New Jersey

RAYMOND T. PIERREHUMBERT

Geophysical Fluid Dynamics Laboratory/NOAA, Princeton University, Princeton, New Jersey

(Manuscript received 1 September 1987, in final form 8 April 1988)

ABSTRACT

The effect of Ekman friction on baroclinic instability is reexamined in order to address questions raised by Farrell concerning the existence of normal mode instability in the atmosphere. As the degree of meridional confinement is central to the result, a linearized two-dimensional (latitude–height) quasi-geostrophic model is used to obviate the arbitrariness inherent in choosing a channel width in one-dimensional (vertical shear only) models. The two-dimensional eigenvalue problem was solved by pseudospectral method using rational Chebyshev expansions in both vertical and meridional directions. It is concluded that the instability can be eliminated only by the combination of strong Ekman friction with weak large-scale wind shear. Estimates of Ekman friction based on a realistic boundary-layer model indicate that such conditions can prevail over land when the boundary layer is neutrally stratified. For values of Ekman friction appropriate to the open ocean, friction can reduce the growth rate of the most unstable mode by at most a factor of two but cannot eliminate the instability.

By reducing the growth rate and shifting the most unstable mode to lower zonal wavenumbers, viscous effects make the heat and momentum fluxes of the most unstable mode deeper and less meridionally confined than in the inviscid case. Nevertheless, linear theory still underestimates the penetration depth of the momentum fluxes, as compared to observations and nonlinear numerical models.

1. Introduction

Baroclinic instability has long been the subject of extensive study in dynamic meteorology, and the instability is generally believed to be the dominant source of midlatitude synoptic-scale transient eddy activity in the Earth's atmosphere. The groundbreaking work by Charney (1947) and Eady (1949) neglected frictional effects, and the most natural way to rectify this deficiency within the framework of quasi-geostrophic theory is to add an Ekman boundary layer at the ground (and lid, if there is one). Because the Ekman pumping can catalyze the release of mean-flow potential energy in addition to damping kinetic energy, the net effect on the instability is not straightforward.

Holopainen (1961), Barcilon (1964) and Williams and Robinson (1974) considered either Phillips-type two layer models or Eady-type models subjected to the influence of one or two Ekman friction layers. They found that if both Ekman layers were present the growth rate was reduced as expected and a long-wave cutoff was also produced (for Eady-type models). However, the presence of a single Ekman layer has a destabilizing effect on the short waves. This destabilizing feature should be recognized as the side effect of the upper rigid lid in their models; if the Ekman layer is at the ground, for example, the destabilized inviscid mode is the *top-trapped* mode, which has no counterpart in the semi-infinite domain. The potential destabilizing effect of a single weak Ekman layer is most readily assessed in terms of the pseudomomentum formulation described in Held et al. [1986, see esp. Eq. (9)] for the continuous case and Panetta et al. (1988) for the two layer case. Briefly, only inviscid neutral modes with pseudomomentum of the same sign as the Doppler-shifted phase speed at the ground $[c - u(0)]$ are destabilized by the introduction of a weak lower Ekman layer. Such modes do not occur in more realistic models, such as the Charney model.

Card and Barcilon (1982) considered the Charney model with an Ekman layer at the lower boundary. In this case the presence of Ekman friction at the lower boundary leads to a significant reduction in growth of disturbances of all wavelengths and the formation of a short-wave cutoff. Inspired by the possibility that Ekman damping could eliminate the normal mode baroclinic instability altogether, Farrell (1985) used Charney's and Eady's models to carry out further studies on baroclinic instability with Ekman damping, both

Corresponding author address: Shian-Jiann Lin, Geophysical Fluid Dynamics Laboratory, Princeton University, P.O. Box 308, Princeton, NJ 08542.

from the normal mode and initial value standpoint. In his model, the flow field was confined to a narrow (1500 km wide) β-channel. Based on his calculations Farrell conjectured that "exponential (normal mode) instability is insignificant or nonexistent when Ekman damping corresponding to moderate values of vertical diffusion (eddy viscosity) is included." Farrell's results are not definitive, however, because he computed the stabilization threshold for only a single channel width and zonal wavenumber. The choice of channel width is crucial, because a narrow channel yields a large total wavenumber, and shortwave perturbations, being shallow, are strongly damped. In determining whether Ekman friction can suppress baroclinic instability in the real atmosphere, the central issue is the degree of meridional confinement occurring in nature. We shall take up this question by using a one-dimensional model with various channel widths and values of Ekman damping, and a two-dimensional model with varying values of shear parameter and Ekman damping. Our estimates of Ekman friction will be based on computations performed with a realistic boundary-layer model. The effects of the Ekman damping on the vertical structure of the unstable waves are also discussed.

2. Formulation

The mathematical formulation of the linearized quasi-geostrophic baroclinic instability problem is documented in Pedlosky (1982); we shall follow his treatment and notation closely. We linearize the quasi-geostrophic β-plane equations about a compressible isothermal atmosphere with wind profile $u(y, z)$ and assume the small disturbances take the form of normal modes, i.e.,

$$\psi(x, y, z, t) = \mathrm{Re}\{\phi(y, z)e^{i(kx-\omega t)}\}e^{z/2}. \quad (1)$$

Also from the basic thermodynamic relations the density scale height $H = RT_0/g$ and Brunt–Väisälä frequency $N = g/(C_pT_0)^{1/2}$ are constants since they are determined solely by the prescribed constant basic state temperature T_0. Therefore, if we adopted the radius of deformation $L_d = NH/f_0$ as our length scale, we obtain the following dimensionless equation which governs the motion of the small disturbances:

$$(u - c)\left[\phi_{yy} + \phi_{zz} - \left(k^2 + \frac{1}{4}\right)\phi\right] + \frac{\partial Q}{\partial y}\phi = 0 \quad (2)$$

where

$$\frac{\partial Q}{\partial y} = \beta - u_{yy} - u_{zz} + u_z \quad (3)$$

is the meridional potential vorticity gradient.

The velocity scale used here is $Hu_z(0, 0)$, where $u_z(0, 0)$ is the vertical shear at the ground and at latitude 45°N, c is the complex phase speed and the dimensionless "beta" parameter is

$$\beta = \frac{\beta_{\mathrm{dim}}L_d^2}{Hu_z(0, 0)}. \quad (4)$$

The Ekman friction is incorporated into the dynamics through the action of Ekman pumping, i.e., by introducing a vertical velocity (which is proportional to the relative vorticity at the edge of the Ekman layer) at the lower boundary. Therefore, the linearized lower boundary condition becomes

$$c\left(\phi_z + \frac{1}{2}\phi\right) + u_z\phi = i\frac{E_v^{1/2}}{2k\epsilon}(k^2\phi - \phi_{yy}), \text{ at } z = 0 \quad (5)$$

where $E_v = 2\nu/f_0H^2$ is the Ekman number and $\epsilon = Hu_z(0, 0)/(f_0L_d)$ is the Rossby number. Together with the energy-decay condition

$$\phi \to 0 \quad \text{as} \quad z \to \infty \quad (6)$$

Eqs. (2) and (4) define the dispersion relation $\Omega(\pi; k, \omega)$ where π represents all the mean flow properties including the eddy viscosity ν.

Care must be taken in determining the mean flow parameters such as the Brunt–Väisälä frequency and the eddy viscosity. In order to be consistent with the isothermal assumption, the Brunt–Väisälä frequency should be calculated directly from the basic state temperature or vice versa rather than be prescribed arbitrarily. From data given in Oort and Rasmusson (1971) it may be inferred that the Northern Hemisphere mean tropospheric temperature at latitude 45°N is about 250 K. The Brunt–Väisälä frequency is then approximately 0.02 s^{-1}, which is somewhat higher than that used in most previous baroclinic instability studies. The choice of the value of vertical eddy viscosity is more controversial. In order to bring some precision and objectivity to bear on this issue, we have carried out computations of Ekman pumping using a boundary layer parameterization based on that in use at the European Centre for Medium Range Weather Forecasting. A complete discussion of the calculation is given in the Appendix. (The reader is urged not to succumb to the temptation to skip this material simply because it has been relegated to an appendix; in some ways, these estimates are at the heart of our argument.) The effective diffusivity varies with boundary layer wind, shear, stratification and surface characteristics, and a variety of cases are discussed in the Appendix. In brief, neutrally stratified boundary layers over the open ocean yield values in the range 1–5 $m^2 s^{-1}$ (oceanic boundary layers with appreciable stable stratification may be regarded as essentially inviscid). Over flat land, neutral conditions yield diffusivities as high as 50 $m^2 s^{-1}$, though moderate stable stratification brings the diffusivity back down to order of 5 $m^2 s^{-1}$. In *mountainous* terrain, the model can yield diffusivities of 20 $m^2 s^{-1}$ or more even in the presence of strong stable stratification, but this estimate

must be regarded as suspect owing to the rather primitive state of development of boundary layer theory in steep orography.

Apart from any imprecision of the estimate of boundary layer diffusivity, there are errors inherent in assuming Ekman boundary-layer dynamics and in linearization of the damping—in linear theory, $E_v^{1/2}$ is constant, whereas in reality the growth of the perturbation surface wind will soon dominate the relatively weak mean surface wind, leading to growth of the surface stress and hence enhanced (but spatially and temporally varying) Ekman damping. A saving grace is that the diffusivity appears in (5) only in the form $E_v^{1/2}$, so that the sensitivity is not extreme. We further hedge our bets by carrying out calculations for a range of diffusivities about the "best guess."

3. One dimensional model

Equation (2) is a nonseparable partial differential equation which will be solved in section 4 by a recently developed numerical scheme. A great simplification can be achieved by ignoring the meridional variation of the mean flow and assuming that the small perturbations are sinusoidal in y-direction, i.e., replacing $\phi(y, z)$ by $\phi(z)e^{ily}$ everywhere. To accomplish this, two meridional walls are assumed to confine the waves. Equation (2) now becomes an ordinary differential equation, which is easier to solve.

It is possible to obtain the dispersion relation for large $K^2 \equiv k^2 + l^2$ by a straightforward extension of the short-wave expansion described in Pierrehumbert (1986) allowing for the Ekman term in the lower boundary condition. For large K the solution of (2) is $\phi = e^{-Kz+ily}$. Substituting in the boundary condition (5) then yields

$$\omega = -i\frac{E_v^{1/2}}{2\epsilon}K + O(1).$$

Thus, there is a unique eigenmode at short wavelengths, and it is highly damped. This remark constitutes a simple proof that any Ekman friction introduces a short-wave cutoff, and applies regardless of the form of $U(y, z)$, so long as $\partial Q/\partial y$ is finite.

Using the shooting method together with an analytic continuation technique such as employed in Pierrehumbert (1986), this solution can be continued back to the long-wave side. However, we found that the (unique) short-wave mode continues into a highly damped mode rather than the Ekman-modified unstable mode, which is of primary interest. This suggests that, at least in the one-dimensional case, the unstable mode disappears at the stability boundary rather than crossing over into a damped mode. In any event, this complication makes it difficult to find the unstable modes by continuing from known analytical solutions. The shooting method is fast and accurate, but lack of a systematic method of generating initial guesses is apt to miss physically important modes. To remedy this problem a global method must be used. We adopted the transformation technique developed in Boyd (1987) to transform the Chebyshev polynomials to the "rational Chebyshev series" then used it as the basis functions for spectral expansion; full details are given in section 4.

The one-dimensional wind profile we use here is

$$u(z) = ze^{-z^2/4.5} \tag{7}$$

and is illustrated in Fig. 1 along with Charney profile. This wind profile has the same shear as the Charney profile at the ground and has a maximum wind at the height of tropopause ($1.5H = 10.5$ km) then it decays to zero at infinity. The basic parameters are

$$N = 0.02\ \text{s}^{-1},\quad H = 7\ \text{km},\quad L_d = 1400\ \text{km},$$

$$u_z(0) = 35\ \text{m s}^{-1}/7\ \text{km}\quad \text{and}\quad \nu = 3.6\ \text{m}^2\ \text{s}^{-1}.$$

Note that the value of eddy viscosity used here represents a moderate Ekman friction, characteristic of a neutral boundary layer over open ocean or a stably stratified boundary layer over land (see Appendix). The maximum wind corresponding to the shear value given above is about 32 m s^{-1}.

Figures 2a and 2b show the growth rate and phase speed of the unstable mode for the Charney model without Ekman friction and for our modified 1D model with and without friction. Here the meridional wavenumber l was set to zero (the most unstable case) for simplicity. As is well known, the deviations from the

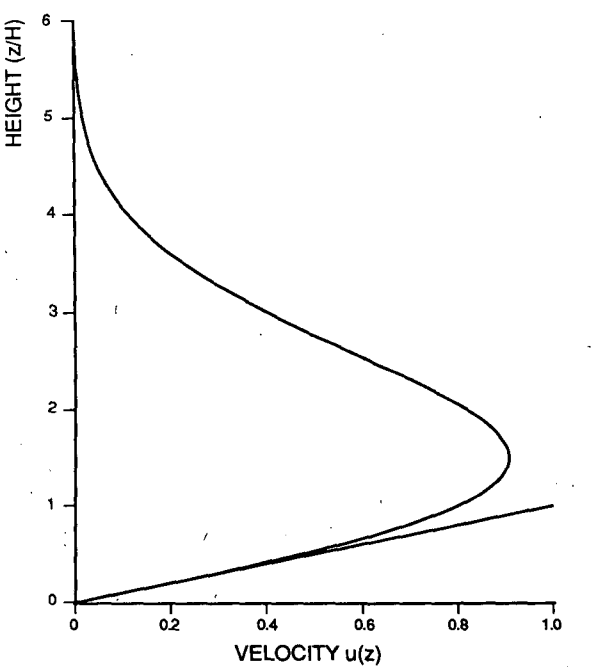

FIG. 1. The wind profile $u(z)$ used in the 1D model. The straight line is the Charney profile. The vertical shear at the ground level in both profiles are the same.

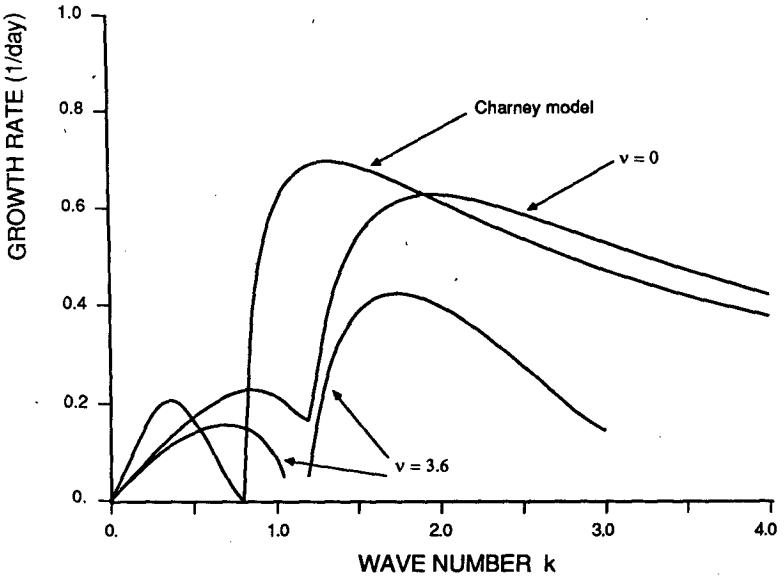

FIG. 2a. The growth rate as a function of wavenumber k for Charney model without friction, the one-dimensional jet profile with $\nu = 3.6\ m^2\ s^{-1}$ and the same profile without friction. The vertical shear at the ground is $5 \times 10^{-3}\ s^{-1}$.

Charney profile eliminate the neutral point separating Green modes from Charney modes. As expected from the arguments of Pierrehumbert (1986) the inviscid short-wave behavior of our model is asymptotic to that of Charney's model as k goes to infinity, since the short-wave behavior depends only on the shear at the ground. The inclusion of Ekman friction reduces the growth rate everywhere for the internal jet model, just as Card and Barcilon (1982) found to be the case for the Charney model.

From Fig. 2b, it is seen that the Ekman friction somewhat retards the phase speed of the unstable mode. By definition, c is real at a stability boundary, and the indication in Fig. 2b is that c_r remains positive as the growth rate approaches zero. Because the Ekman friction appears only in the bottom boundary conditions, the viscous effects do not desingularize the critical level, and the mode at the stability boundary would appear to have a logarithmic singularity where $U = c_r$. Because the singularity cannot be resolved with a finite number

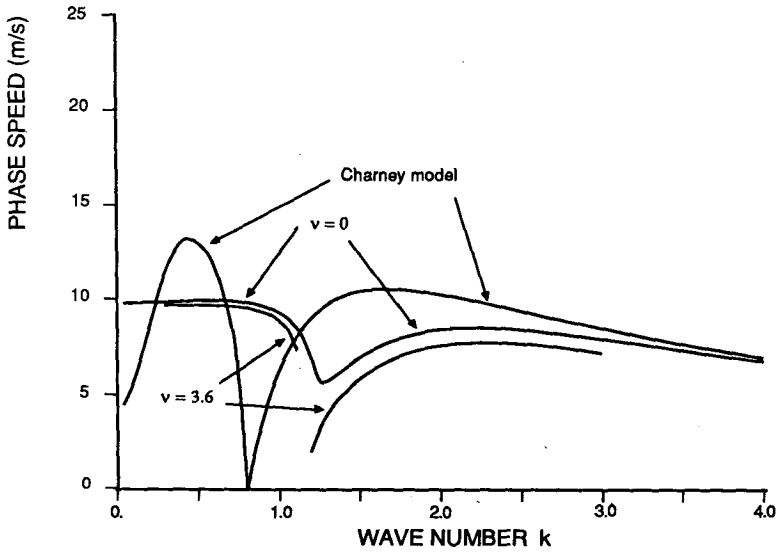

FIG. 2b. As in Fig. 2a, but for the phase speed.

of degrees of freedom, convergence is poor near the stability boundary, and it is difficult to accurately compute the growth rates there. For the same reason, it is difficult to pin down precisely the position of the stability boundary using numerical methods alone, or indeed to demonstrate convincingly that a stability boundary exists at all. The pure Charney model is not plagued by this problem, as the stability boundary separating Green and Charney modes has its critical level only at the ground, and in consequence is not singular. For whatever it is worth, our calculations suggest a short-wave cutoff for k somewhat greater than 3.0, and also indicate that there may be a small stable gap between the Green and Charney modes in the dissipative case. In any event, our main concern in this paper is not with the behavior near stability boundaries, but with the growth rate of the most unstable mode, for which convergence is not a problem.

Now we focus our attention on the effect of change in meridional scale and eddy viscosity on the maximum growth rate. Figure 3 was the result of an extensive numerical study covering the whole plausible range of ν (from 0 to 100 $m^2 s^{-1}$) and streamwise wavenumber k for three different values of l seeking for the maximum growth rate in each case. The result for the case $l = 2$ is the closest one to that of Farrell, although he did not allow k to vary. In this particular case, the instability indeed is insignificant if ν is larger than 4.5 $m^2 s^{-1}$. However, the results from the other two cases reveal that even at $\nu = 100$ $m^2 s^{-1}$ the instability is not insignificant. This tells the whole story about the importance of the meridional scale in this problem. The lesson here is that one must be very careful in choosing all the parameters and length scales in order to render the one-dimensional model meaningful. Needless to say, this requires profound physical insight and perhaps some good luck. The solution to this dilemma is to use the full two-dimensional model with two-dimensional jetlike wind profile and let the nature of the jet determine the proper meridional scale of unstable waves.

4. Two-dimensional model

In order to make the comparison with our 1D models meaningful and still capture the main features of the real atmosphere, we adopt the following profile

$$u(y, z) = \operatorname{sech}^2(y) z e^{-z^2/4.5}. \tag{8}$$

It is symmetric about $y = 0$ (latitude 45°N) and decays to zero at infinity. The contour plot of this wind profile on the meridional section (y–z plane) is shown in Fig. 4. When $\epsilon = 0.25$ the corresponding dimensional wind has vertical and horizontal shear comparable to the observed *zonal mean* wind; a value $\epsilon = 0.5$ might be more typical of shears encountered in the oceanic storm tracks.

Insertion of this wind field into (2, 5) yields a two-dimensional eigenvalue problem, which we will solve by spectral discretization followed by truncation to a finite-dimensional algebraic eigenvalue problem. The spectral and pseudospectral methods have been widely used in numerical modeling of fluid flow. Until recently it has been applied only to bounded or periodic domains. Using the usual basis functions in an infinite domain (y-direction) or semi-infinite domain (z-direction) one encounters the difficulty of satisfying the boundary conditions at infinity. Grosch and Orszag (1977) employed both algebraic and exponential map-

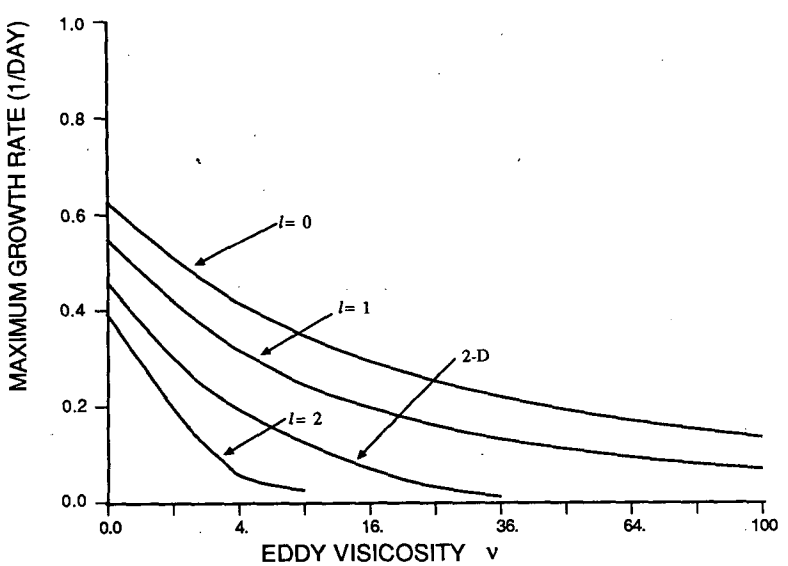

FIG. 3. Maximum growth rate as a function of vertical eddy viscosity for 1D model, $l = 0$, 1, 2 and 2D model. Both 1D and 2D models have the same Rossby number $\epsilon = 0.25$, based on maximum vertical shear at the ground.

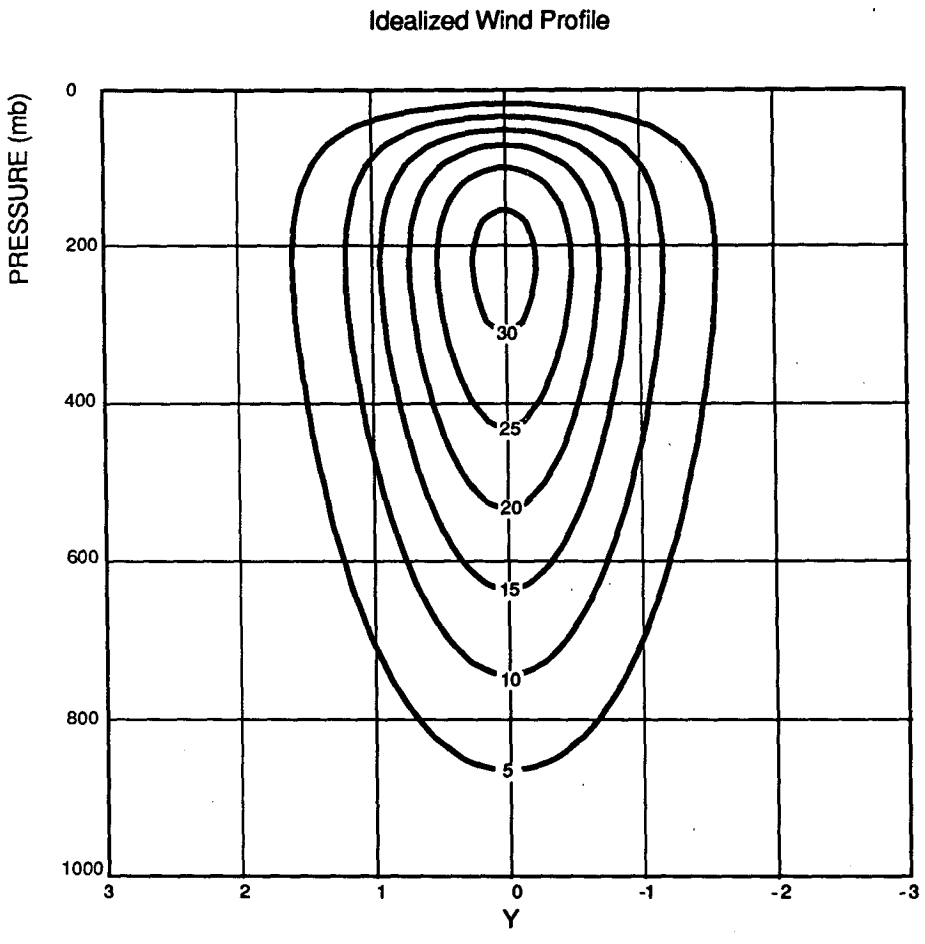

FIG. 4. The wind profile used in the 2D model, $u(y, z) = \text{sech}^2 y\, ze^{-z^2/4.5}$. The contour labels give dimensional wind speeds in m s^{-1}, corresponding to $\epsilon = 0.25$. y and z are nondimensionalized by the radius of deformation L_d and density scale height H respectively.

pings to solve some fluid dynamics problems in semi-infinite domain with success. Instead of transforming the infinite or semi-infinite physical domain into a bounded computational domain as Grosch and Orszag did, Boyd (1987a,b) employed an algebraic transformation to transform the Chebyshev polynomials directly. The advantage of Boyd's method is that we do it once for all time and the equations need not be changed. The mechanisms to do the transformations in both the vertical (semi-infinite domain) and meridional direction (infinite domain) are described in detail in Boyd's two recent papers, each in the context of the one-dimensional problem. We employed these two techniques in our problem simultaneously, and call it *double Chebyshev expansion.* Let

$$\phi(y, z) = \sum_{n=0}^{N} \sum_{m=0}^{M} X_{mn} TB_m(y) TL_n(z) \qquad (9)$$

where TB and TL are the transformed Chebyshev polynomials–rational Chebyshev series (see Boyd 1987a,b) in y and z respectively. Here M and N are the number of expansion terms, representing the meridional and vertical resolution, respectively. As described by Boyd, the infinite horizontal domain is implicitly transformed to the finite interval using $y = Ly'/(1 - y'^2)^{1/2}$, and the semi-infinite vertical domain is transformed using $z = L(1 + z')/(1 - z')$; for both transformations we used $L = 1$.

Note that this representation of the function $\phi(y, z)$ satisfies the decay condition (6) naturally. Since the wind profile is symmetric about y, so is the governing equation; therefore we need only half of the basis functions (in the y direction) to achieve the same accuracy as in the general case. To set up the pseudospectral matrix, we chose the evenly spaced pseudogrids (collocation points) in the Fourier-space such that in the real physical-space they are concentrated near the ground and near the center of the jet. Substituting (9) into (2) and the lower boundary condition (5) then rearranging terms, we obtain a generalized eigenvalue problem of the form

$$\mathbf{A}\bar{\mathbf{X}} = c\mathbf{B}\bar{\mathbf{X}} \qquad (10)$$

TABLE 1. Matrix size and CPU time requirement for the 2-D model.

Resolution ($M \times N$)	Matrix size	CPU time (sec)
10×20	200×200	84
12×24	288×288	232
14×28	392×392	590

where **A** and **B** are (MN) by (MN) matrices determined by the mean flow properties and wavenumber k, c is the complex phase speed (eigenvalue) and $\bar{\mathbf{X}}$ is the eigenvector. Equation (10) can be readily solved by the IMSL subroutine EIGZC or other standard packages.

To solve the two-dimensional model is very expensive compared to of the 1D models. While the 1D models can be easily solved—even on a personal computer, the requirement of CPU time and memory of the 2D model made it prohibitive to run very many cases—even on a Cyber 205. Table 1 lists the CPU time required for three different resolution on a two-pipe Cyber 205, using the IMSL routines in 64-bit precision. The CPU time required is approximately proportional to the cube of the matrix size, indicating that the vector speed-up has already saturated for matrices of order 200.

The modes in a system with symmetric jet profile can be classified as symmetric or antisymmetric, and each class can be computed separately. Since we are mostly concerned with growth of the most unstable waves, and the growth rates of the antisymmetric modes were found to be always smaller than that of the symmetric modes, we will show the results for the most unstable symmetric mode only.

Generally speaking, the convergence rate of this spectral expansion is strongly related to the "degree of singularity" of Eq. (2). In case of strong instability (less singular), we found that the resolution 10×20 gives almost identical results to that of the higher resolution 14×28. However, it gives poor results near the stability boundary. In all of the results presented here, we used a 12×24 resolution for most of the calculations except near stability boundary where a 14×28 resolution was used.

The Rossby number ϵ in this problem is a measure of wind shear, e.g., $\epsilon = 0.25$ is the case where maximum wind at the tropopause is about 32 m s^{-1} (the mean wintertime value, referred to hereafter as typical wind shear) and $\epsilon = 0.5$ corresponds to a maximum wind about 64 m s^{-1} (hereafter referred to as strong wind shear). We regard eddy viscosity 3.6 m^2 s^{-1} as the normal friction and 36 m^2 s^{-1} as a strong friction in the Ekman layer (see the Appendix).

Figure 5a is the plot of growth rates versus wavenumber k for four cases. The case with $\epsilon = 0.25$ and $\nu = 3.6$ (typical wind shear and normal friction) should represent the real atmosphere rather well. The e-folding time of the most unstable wave is close to 5 days and the most unstable wavelength is about 4400 km ($k \approx 2.0$) which is close to the observed scales of the synoptic cyclones. The maximum growth rate for the case with $\epsilon = 0.5$ and $\nu = 36.0$ (strong shear and strong friction) is much higher than that of the case with typical shear and normal friction. In other words, a twofold increase in wind shear can easily overcome a tenfold

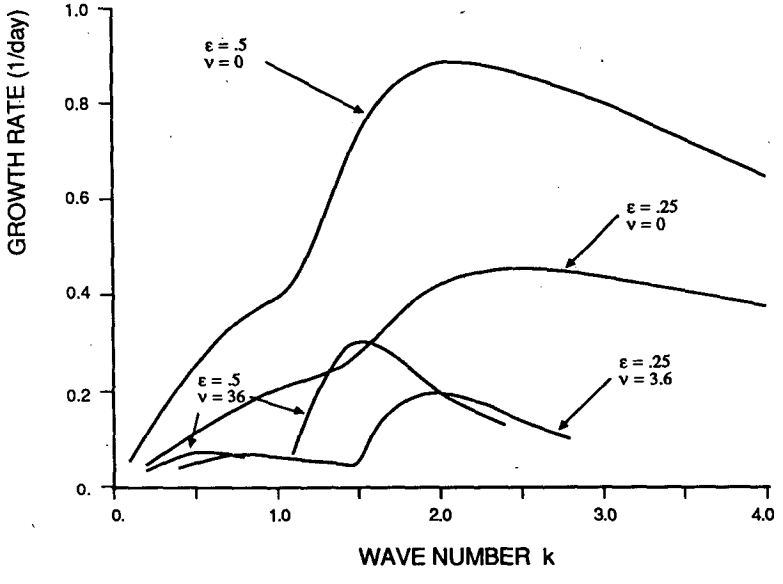

FIG. 5a. The growth rates plotted as a function of wavenumber k, for the most unstable mode in the two dimensional model. ϵ is the Rossby number, which is a measure of wind shear and ν is the vertical eddy viscosity.

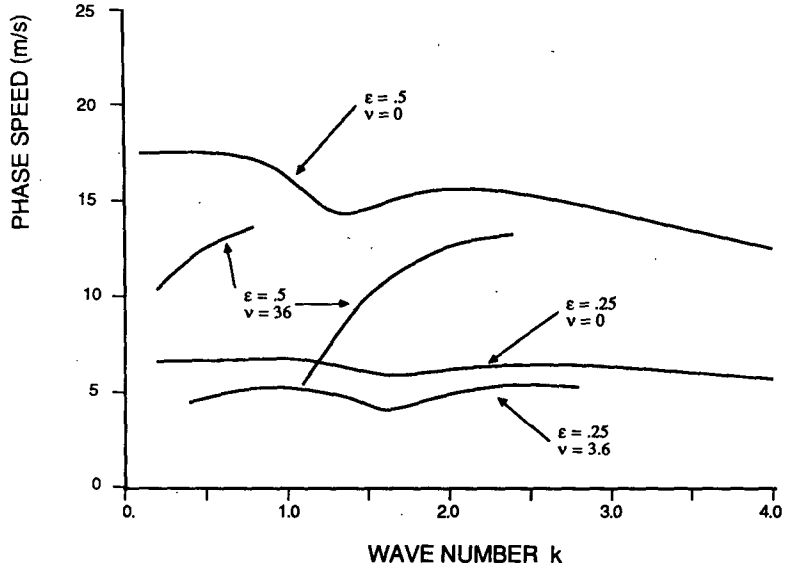

FIG. 5b. As in Fig. 5a, but for the phase speed.

increase in eddy viscosity on the effect of the growth of unstable waves. This result arises primarily from the fact that the friction enters the nondimensional equation (5) only in the combination $E_v^{1/2}/\epsilon$ so that the *nondimensional* growth rates are only slightly reduced in the strong friction/strong shear case; this is more than offset by the doubled shear against which the growth rates are redimensionalized. Increasing the shear also affects the problem via a reduction of β, but the contribution of this effect to the change in maximum growth rate is not very great. In any event, it is clear that dissipative suppression of baroclinic instability in the oceanic jets is highly unlikely, as the instability can still grow vigorously even if we use the "normal shear" for the wind profile (which is an underestimate of the actual shear) and friction values characteristic of a neutrally stratified boundary layer (which is an overestimate of the dissipation).

The problem with using the classic one-dimensional model is that it is difficult to pick an appropriate value of meridional wavenumber to properly represent the actual meridional scale of the unstable waves. As an indication of the degree of meridional confinement in the 2D model, we have plotted the maximum growth rate for the normal shear case versus eddy viscosity in Fig. 3 in addition to the 1D results. We see that the magnitude of the *effective* meridional wavenumber in the 2D model is between 1 and 2 (in units based on radius of deformation), and that the slight decrease in effective wavenumber over that chosen by Farrell necessitates a much larger friction for stabilization.

Two inviscid cases were also studied for comparison with the viscous cases and some previous studies. The WKB approximation used by Ioannou and Lindzen (1986) to study the instability of two-dimensional jets is very promising; it reproduces the salient predictions of the full two-dimensional inviscid calculation quite well. The WKB approximation provides a systematic way to choose the proper *complex* meridional wavenumber. Although the technique is formally limited to jets with broad meridional structure, comparison with our full two-dimensional results attests to its robustness. The success of WKB may be due to the strong meridional trapping of the mode at the latitude of the jet maximum, as will be exhibited shortly. Ioannou and Lindzen did not include Ekman friction in their calculation, but we expect that the agreement would be similarly good in the damped case.

Considerable discrepancy was found with the numerical results of Gall (1976), particularly for the short waves. The short waves exhibit a very high rate of growth in his model. The discrepancy may perhaps be attributed to the poor resolution and insufficient nonlinear viscosity (of the type introduced by Smagorinsky 1963) to control the "computational mode" in Gall's GCM-like model. This point of view is supported by the result from a high-resolution spectral model by Young and Villere (1985). They also used the primitive equations in spherical geometry but adopted a horizontal scale-selective damping instead to prevent energy accumulation in the smallest resolved scales and did not include any mechanism for surface friction. Their result is generally consistent with our result for normal wind shear without friction. For a jet at 45° latitude, they find a maximum growth rate of 0.5 day^{-1} (vs 0.46 for the quasi-geostrophic model) occurring at zonal wavenumber 9, which is roughly equivalent to $k = 3$ in our units (vs maximum growth near $k = 2.5$ in quasi-geostrophic theory). The chief difference is that Young and Villere's growth rate falls off much

more steeply with increasing wavenumber than does the inviscid quasi-geostrophic result; we do not know whether this is due primarily to the scale-selective damping or to ageostrophic effects. The basic state wind profiles used in Gall, Ioannou and Lindzen, and Young and Villere's models are all very similar to ours (the maximum wind speeds are all around 32 m s^{-1}) although they differ in details. The general similarity between the quasi-geostrophic β-plane results and the spherical primitive-equation results suggests that the former approximation is an adequate framework for addressing the effects of Ekman friction in the real atmosphere.

The phase speeds for the four cases are shown in Fig. 5b. As in the 1D model, the phase speed was reduced by the friction. In the 2D case, it is rather insensitive to zonal wavenumber, except when the friction is strong. Also as in the 1D case, the results lead one to speculate that the stability boundary occurs at positive c, and hence is associated with a singular mode. The numerical methods employed here are not really adequate for addressing issues related to the stability boundary, however.

We also carried out a calculation for the case with normal wind shear ($\epsilon = 0.25$) and strong friction ($\nu = 36$ m^2 s^{-1}). The growth rates were found to be neg-

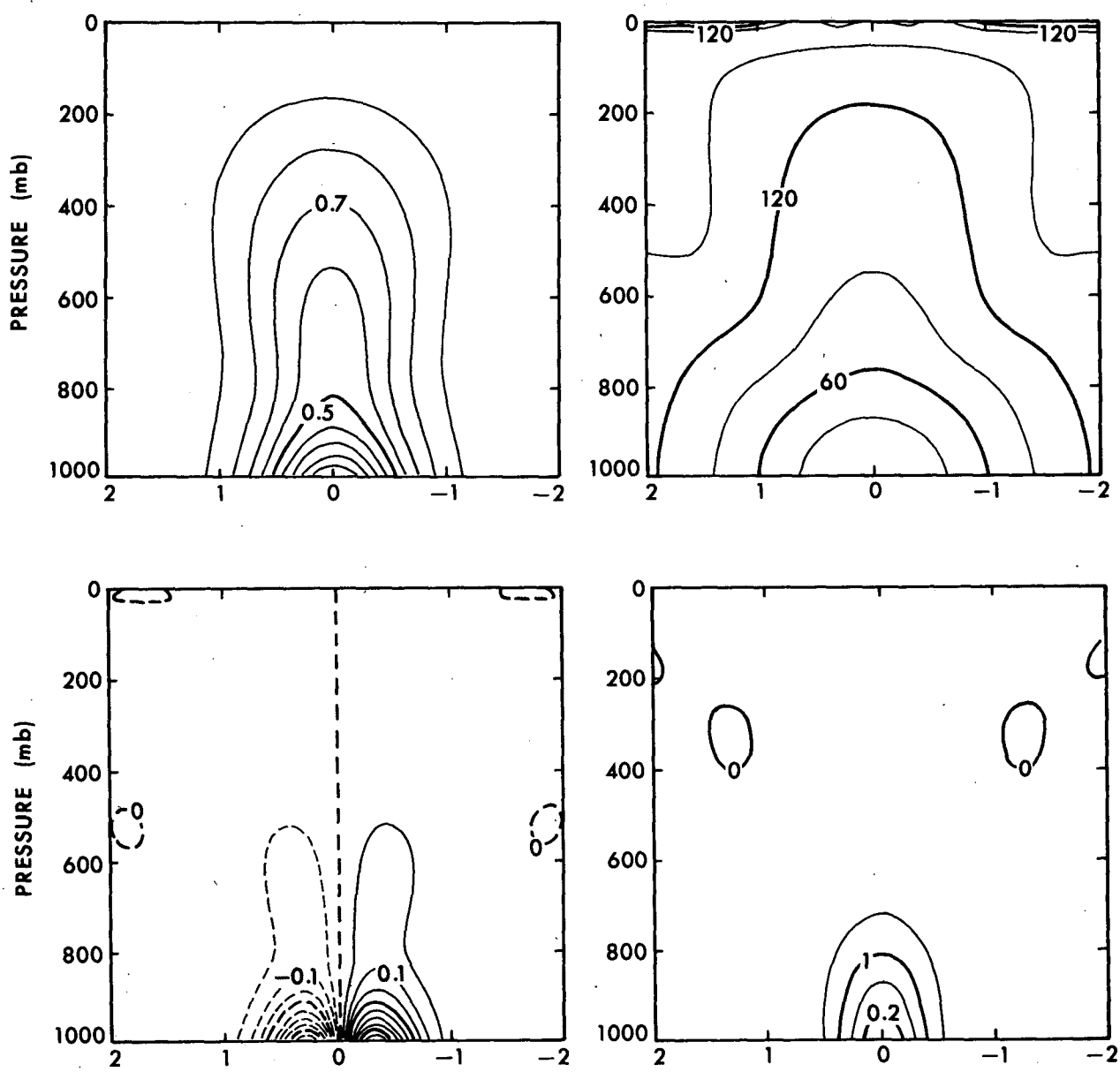

FIG. 6. Upper left panel: The wave amplitude $|\phi|$. Upper right panel: The phase angle in degree. Lower left panel: Momentum flux $\rho\overline{u'v'}$. Lower right panel: Heat flux $\rho\overline{v'\theta'}$. Results are for the case with $\epsilon = 0.25$, $\nu = 0$ and $k = 2.0$.

ligibly small. Owing to convergence problems, we cannot say with certainty whether the growth has been eliminated or merely reduced to a very small value; however, for all practical purposes, this case may be regarded as baroclinically stable. As shown in the Appendix, the friction used here is typical of a neutrally stratified boundary layer over land. Combined with the fact that the normal wind shear is perhaps slightly stronger that the magnitude typically found away from the oceanic jet maxima, it appears likely that circumstances can arise in which baroclinic instability is eliminated over the continents. The main factor preventing this state of affairs from prevailing is the generally stable stratification of the boundary layers.

There are two well-known deficiencies in the linear baroclinic instability theory. First, the wavelength of maximum growth predicted by linear theory is somewhat shorter than the observed scales of baroclinic energy release in the atmosphere. Second, while the observations show a primary maximum of eddy kinetic energy near the tropopause with only a secondary maximum at ground level, the linear theory invariably predicts a primary maximum at the ground except for ultralong waves, which are only weakly unstable. These discrepancies are generally attributed to nonlinear effects. We have already shown that with the inclusion of Ekman friction the most unstable wavelength can be lengthened. In the following we will also show what

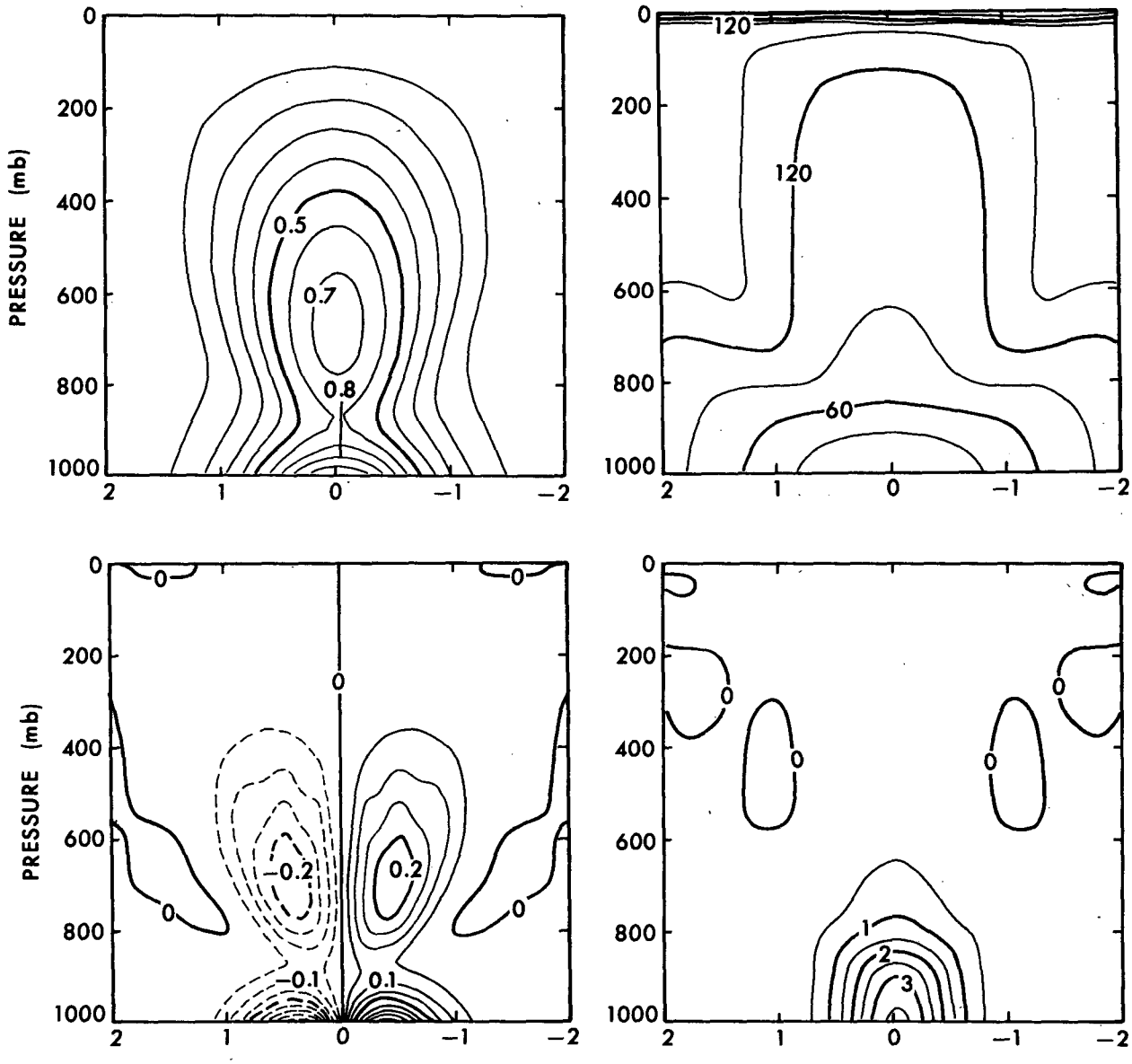

FIG. 7. Same as Fig. 6, but for the case with $\epsilon = 0.25$, $\nu = 3.6\ \mathrm{m^2\ s^{-1}}$.

the Ekman friction can do to improve the second deficiency of the linear theory.

The contour plot of the wave amplitude, phase, momentum and heat fluxes on a meridional section are shown in Figs. 6–8 for a variety of flow configurations at a fixed wavenumber $k = 2.0$ (corresponding wavelength is about 4400 km). Note that all of these patterns are symmetric about 45°N (since this is a symmetric mode).

Figures 6a–d are for the case with typical wind shear and no friction. The prominent features of this inviscid case are: The amplitude, momentum and heat fluxes are all concentrated near the ground level and the central portion of the jet and there is no secondary maximum aloft. The "steering level" is now a curved surface with the lowest level at 45°N instead of a flat one in the 1D model. The momentum fluxes are all countergradient except for two very small regions as shown in the figure. The phase shows westward tilt in most of the domain so the heat fluxes are mostly northward. These pictures bear a remarkable resemblance to the results (of the first symmetric mode with wavelength 4000 km) found in Ioannou and Lindzen (1986). The WKB approximation again seems to capture much of the behavior of the full two-dimensional problem.

Figures 7a–d are for the same wind shear as in the first case but including a normal friction. The Ekman friction has made some improvement here; the wave

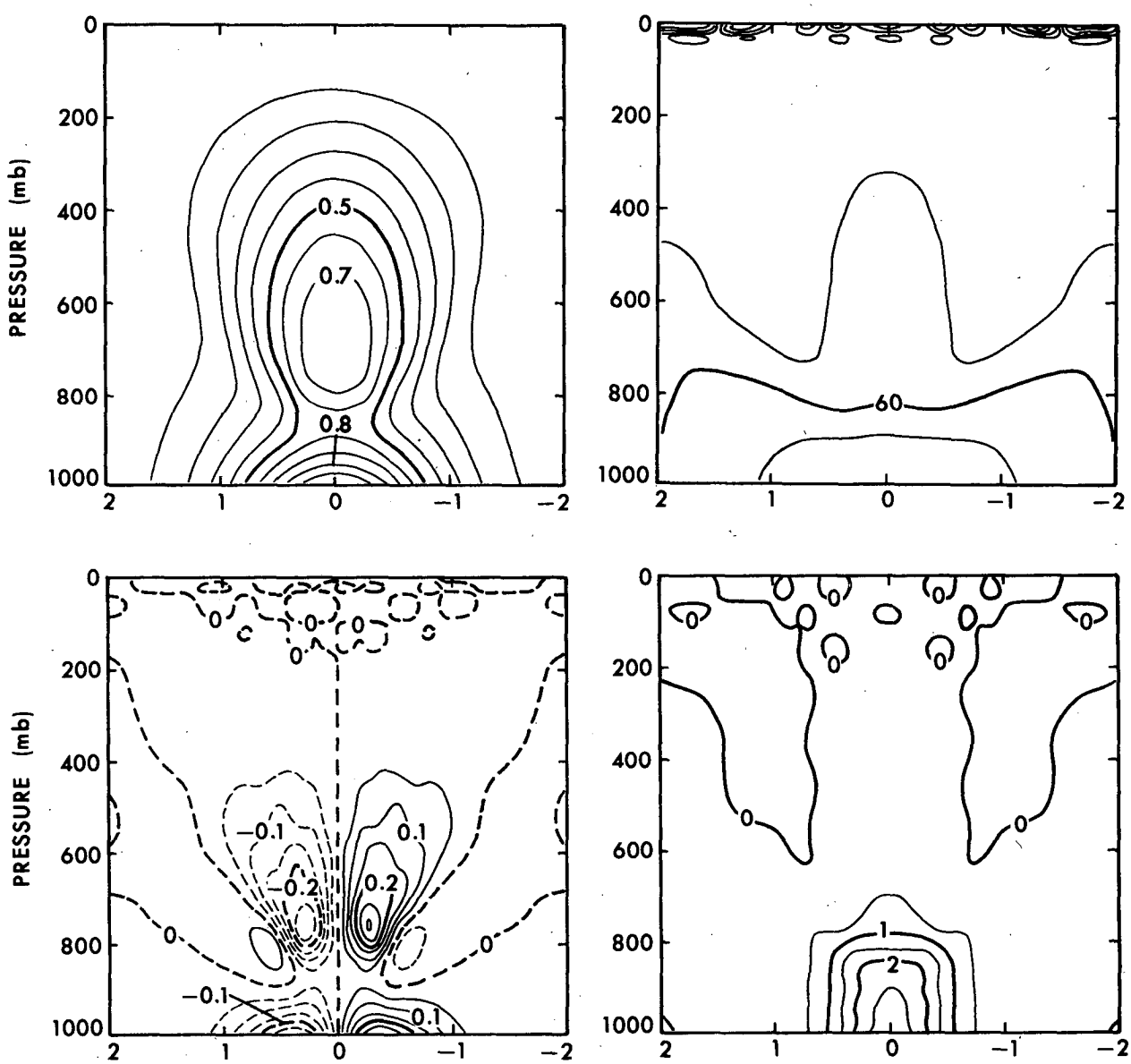

FIG. 8. As Fig. 6, but for the case with $\epsilon = 0.5$, $\nu = 36.0\ \mathrm{m^2\ s^{-1}}$.

amplitude has now developed a secondary maximum near the 700 mb level and so has the momentum flux. The portion of downgradient momentum and equatorward heat flux in the meridional section were also increased. The case with strong shear and strong friction is shown in Figures 8a–d. The region where we have downgradient momentum flux and equatorward heat flux is further increased, and the secondary maximum of wave amplitude and momentum flux is stronger as compared with the normal friction case. Despite the improvement in penetration of the momentum fluxes, the level of the maximum still falls far short of the 300 mb level typically encountered in both observations and nonlinear numerical simulations.

In all these cases, the momentum flux of the linear modes acts to spin up the winds near the surface, and therefore tends to reduce the baroclinic instability of the system; the influence is more effective in the frictional cases, because the fluxes are less bottom-trapped. The momentum fluxes are *upgradient* for the most part, and do not act diffusively.

5. Concluding remarks

We have carried out calculations of the effect of Ekman friction on baroclinic instability, using a nonseparable 2D model to obviate the inherent difficulty in choosing an effective channel width in 1D models, and using a realistic boundary layer model to provide a reliable estimate of Ekman pumping. Our principal conclusion is that Ekman friction almost certainly cannot eliminate baroclinic instability in the oceanic storm tracks; we found that the instability can grow quite vigorously, even subject to a vertical shear estimate which is at the low end of the plausible range and a friction estimate which is at the high end. Over the continents, where the vertical shear tends to be weaker and friction tends to be stronger, suppression of baroclinic instability is within the realm of possibility, but then only if the boundary layer is not appreciably stably stratified. It is worth noting that the oceanic jets are probably *convectively* rather than *absolutely* unstable (Pierrehumbert 1986), so that amplifying wave packets would ultimately leave the highly unstable jet regions and dissipate (or at least grow at a greatly reduced rate) over the continents. The possibility thus emerges that frictional stabilization may contribute to the rather sharp termination of the Pacific and Atlantic storm tracks observed at the continental boundaries.

With the inclusion of Ekman friction at the lower boundary, we get a more realistic upper structure of the unstable waves, and the wavelength of the most unstable wave is lengthened. The geopotential height fluctuation, heat flux and most notably momentum flux all penetrate to considerably greater heights, and the latter develops a secondary maximum aloft. While the vertical distribution of momentum fluxes is still not nearly as deep as that seen in observations and nonlinear numerical simulations, the frictional effects leave a bit less that needs to be accounted for by nonlinear effects associated with saturation and Rossby wave radiation. In a sense, the stabilizing effects of Ekman friction advance the wave somewhat in its life cycle.

Our results demonstrate that the present-day Earth's atmosphere is indeed baroclinically unstable, and hence that transient eddies can be spontaneously generated in the oceanic jet regions. We shall leave unresolved the question of which class of observed phenomena is actually due to such instability, though what we have in mind are storm track transients such as identified in band-pass analyses of Blackmon et al. (1984a,b) and Plumb (1986). These motions have characteristics which are generally in line with those of the normal mode instability, manifested in the form of a wave packet propagating through the storm track. On the other hand, a number of case studies (e.g., Sanders 1987) suggest that vigorous cyclogenesis can commonly occur at much smaller scales. To be sure, a small scale perturbation was posited by Farrell largely to bring the scale of the perturbation in line with that of such cyclones, and our calculation does not contradict his conclusion that normal mode growth *at small scales* (relative to the radius of deformation) is strongly inhibited by Ekman friction. To this remark must be attached two caveats. First, one's subjective impression of the "scale" of a cyclone is dominated by the extent of the region of closed surface streamlines, which is not related in any simple way to the wavelength of the instability that may be the prime mover in the process; moreover, the scale of the mature cyclone is affected by many nonlinear processes (including latent heat release and stretching of relative vorticity) which one should not expect to be captured by a stability analysis. Second, the explosive developments often occur in an environment of effectively weak (moist) static stability. This reduces the radius of deformation L_d which has the dual effect of shifting the maximum growth to shorter dimensional wavelengths (since our length scales are nondimensionalized against L_d) and reducing the effective damping [since reducing L_d increases the Rossby number ϵ, which appears in the denominator of the friction term in (5)]. All this notwithstanding, we would not care to claim that *all* forms of cyclogenesis arise from normal mode baroclinic instability; there remains ample scope for other mechanisms in explaining small scale explosive cyclogenesis.

Acknowledgments. The authors are indebted to Brian Farrell for a number of illuminating communications, and to Erland Källen for some valuable suggestions concerning boundary-layer modeling. R.T.P. is grateful for the hospitality provided by the Meteorological Institute of Stockholm University, where some of the above work was carried out.

APPENDIX

The Estimation of Ekman Friction

Our estimate of the effective Ekman friction is based on a linear Ekman layer model with general height dependent viscosity $\nu(z)$ and a drag law lower boundary condition applied at $z = z_1$. Introducing the complex velocity $\hat{u} = u + iv$, the equations for this model are

$$\frac{d}{dz}\left(\nu(z)\frac{d}{dz}\hat{u}\right) = if(\hat{u} - \hat{u}_g) \tag{A1}$$

subject to boundary conditions

$$\hat{u} \to \hat{u}_g \quad \text{as} \quad z \to \infty \tag{A2}$$

$$\nu(z)\frac{d\hat{u}}{dz} = C\hat{u}(z) \quad \text{at} \quad z = z_1. \tag{A3}$$

The drag coefficient C is obtained by linearizing the surface stress formula $[C_D|u|u]$ about a constant surface wind u_s; thus, $C = 2C_D u_s$. As usual, f is the Coriolis parameter and $\hat{u}_g$ is the geostrophic velocity at the outer edge of the boundary layer.

If $F(z)$ is the solution of the homogeneous form of (A1) (i.e. with $\hat{u}_g$ set to zero) with $F(z_1) = 1$ and which decays as $z \to \infty$, then the vertical velocity at the outer edge of the boundary layer is readily found to be

$$w_1 = \delta_E \zeta_g \tag{A4}$$

where ζ_g is the geostrophic vorticity at the outer edge of the boundary layer and δ_E is the effective Ekman layer depth, given in terms of F by

$$\delta_E = \frac{C}{f}\,\mathrm{Re}\left[\frac{\nu(z_1)\dfrac{dF}{dz}}{\nu(z_1)\dfrac{dF}{dz} - C}\right] \tag{A5}$$

in which the derivatives of F are to be evaluated at $z = z_1$.

To evaluate (A5) it is only necessary to compute $F(z)$ by means of standard techniques of numerical integration. The $F(z)$ depends on strength of the vertical diffusivity but is independent of C. In the limit of large C with fixed diffusivity, the Ekman pumping becomes independent of C and the drag-law boundary condition becomes equivalent to a simple no-slip condition. In the opposite limit the pumping becomes independent of diffusivity and we have $\delta_E = C/f$. It may seem paradoxical that the surface drag effects dominate the pumping precisely when the drag coefficient is small, but this result is readily explained by the fact that the surface drag determines the momentum flux at the bottom of the Ekman layer model, without which there would be nothing for the diffusivity to communicate upward. Note also that the small C results are not really independent of the *presence* of viscosity, as the limit is taken with fixed, nonzero viscosity.

For constant ν with $C = \infty$, (A5) reduces to $\sqrt{\nu/(2f)}$, whence we define the equivalent constant eddy viscosity $\nu_{\text{eff}} = 2(\delta_E)^2 f$. Since the boundary layer affects the interior quasi-geostrophic flow only through the Ekman pumping, instability results pertinent to the general boundary-layer model can be obtained from the results given in the text by simply using ν_{eff} in the computation of the Ekman number.

The objective of a boundary layer parameterization is to obtain $\nu(z)$ and C_D as a function of gross atmospheric characteristics. While the empirical underpinnings for this endeavour are not all that could be desired, they are not totally absent either. For the purpose of our estimates we adopt the parameterization currently in use in the forecast model of the European Centre for Medium Range Weather Forecasts, as described in Louis (1979, 1985) and Louis et al. (1982). This boundary layer model is based on Monin-Obukhov similarity theory and a mixing-length formulation; it has a reasonably good empirical and physical basis, at least for the nonconvecting case. Further, it seems to us that the short-range forecasts produced by the ECMWF could hardly be as accurate as they are if something as fundamental as the Ekman friction were grossly in error.

The parameters entering the boundary layer parameterization are the height z_1 at which (A3) is applied, the wind speed and shear u_s and u_z at z_1, the Richardson number N^2/u_z^2, and the roughness length z_0. In addition, f enters the problem via the Ekman layer model. The results reported below were calculated with $f = 10^{-4}$ and $z_1 = 500$ m; they are not very sensitive to variations in z_1 and so we simply chose a value comparable to that used in the ECMWF model. Over the open ocean z_0 is obtained from the other parameters in a self-consistent way by means of the Charnock formula (as in the ECMWF parameterization). Over land

TABLE A1. Effective diffusivity from ECMWF boundary layer model.

z_0 (m)	Ri	u_s (m s^{-1})	u_z (s^{-1})	ν_{eff} (m^2 s^{-1})
Open ocean	0.0	5.0	.01	0.7
Open ocean	0.0	5.0	.05	0.7
Open ocean	0.0	10.0	.01	3.7
Open ocean	0.0	20.0	.01	17.0
3.	0.0	5.0	.002	12.6
3.	0.0	5.0	.01	32.2
3.	0.0	5.0	.05	52.5
3.	0.0	10.0	.01	65.1
3.	0.5	5.0	.01	3.4
3.	0.5	10.0	.01	8.7
3.	1.0	5.0	.01	1.9
3.	1.0	10.0	.01	5.0
100.	0.0	5.0	.01	124.4
100.	1.0	5.0	.01	17.0
100.	1.0	10.0	.01	19.0

it is specified by the characteristic scale of surface features; a value of 3 m is believed appropriate to urban or disturbed terrain. Over mountains the ECMWF model uses the subgrid-scale orographic height variance to estimate z_0, and this can lead to values of 100 m or more. The use of such large values of z_0 over mountains must be regarded as speculative, since the estimates are not based on particularly firm empirical or theoretical considerations. Results for a variety of conditions are given in Table A1.

Over the open ocean, the effective diffusivity in neutrally stratified boundary layers is quite weak unless gale-force surface winds are assumed; results for stable stratification are even lower. Over moderately disturbed terrain, the diffusivity in neutral conditions can easily reach 50 $m^2\ s^{-1}$, though modest stable stratification reduces this value considerably. The results are rather insensitive to increasing the surface shear beyond 0.01 (with fixed Ri), since the shear primarily effects the magnitude of $\nu(z)$, and the values in question lie in the "small C" regime. Weakening the shear, however, does reduce the effective diffusivity appreciably. Finally, large values of diffusivity are obtained over mountains, even under stably stratified conditions.

We have discussed results only for the nonconvecting case $\mathrm{Ri} \geq 0$. The ECMWF scheme also transports momentum in convecting situations. All other parameters being fixed, the drag and diffusivity in a convecting layer can be an order of magnitude larger than in the neutral case. As noted by the originators of the scheme, though, the momentum transport in this situation is not based on particularly sound or well-verified physical principals; it is generally believed that such transports are of little importance in the model as in convecting situations they "have little shear on which to act" (Louis 1985). However, there may be strongly convecting situations in the model which give rise to spurious suppression of cyclogenesis. On the other hand, the behavior of the parameterization may mimic a real effect, though much more would have to be learned about momentum transport in convecting layers before this could be said with any confidence. The possibility that convective friction offsets some of the more familiar diabatic effects of convection on cyclogenesis—particularly at the small cyclone scales typically of interest in this context—merits further looking into.

REFERENCES

Barcilon, V., 1964: Role of the Ekman layers in the stability of the symmetric regime obtained in a rotating annulus. *J. Atmos. Sci.*, **21,** 291–299.

Blackmon, M. L., Y.-H. Lee and J. M. Wallace, 1984a: Horizontal structure of 500 mb height fluctuations with long, intermediate and short time scales. *J. Atmos. Sci.*, **41,** 961–979.

——, ——, —— and H.-H. Hsu, 1984b: Time evolution of 500 mb height fluctuations with long, intermediate and short time scales as deduced from lag-correlation statistics. *J. Atmos. Sci.*, **41,** 981–991.

Boyd, J. P., 1987a: Spectral methods using rational basis functions on an infinite interval. *J. Comput. Phys.*, **69,** 112–142.

——, 1987b: Orthogonal rational functions on a semi-infinite interval. *J. Comput. Phys.*, **70,** 63–88.

Card, P. A., and A. Barcilon, 1982: The Charney stability problem with a lower Ekman layer. *J. Atmos. Sci.*, **39,** 2128–2137.

Charney, J. G., 1947: The dynamics of long waves in a baroclinic westerly current. *J. Meteor.*, **4,** 135–162.

Eady, E. J., 1949: Long waves and cyclone waves. *Tellus,* **1,** 33–52.

Farrell, B., 1985: Transient growth of damped baroclinic waves. *J. Atmos. Sci.*, **42,** 2718–2727.

Gall, R., 1976: Structural changes of growing baroclinic waves. *J. Atmos. Sci.*, **33,** 374–390.

Grosch, C. E., and S. A. Orszag, 1977: Numerical solution of problems in unbounded regions: Coordinate transforms. *J. Comput. Phys.*, **25,** 273–295.

Held, I. M., R. T. Pierrehumbert and R. L. Panetta, 1986: Dissipative destabilization of external Rossby waves. *J. Atmos. Sci.*, **43,** 388–396.

Holopainen, E. O., 1961: On the effect of friction in baroclinic waves. *Tellus,* **13,** 363–367.

Ioannou, P., and R. S. Lindzen, 1986: Baroclinic instability in the presence of barotropic jets. *J. Atmos. Sci.*, **43,** 2999–3014.

Louis, J.-F., 1979: A parametric model of vertical eddy fluxes in the atmosphere. *Bound.-Layer Meteor.*, **17,** 187–202.

——, Ed., 1985: *Research Manual 3. ECMWF Forecast Model—Physical Parameterization.* European Centre for Medium Range Weather Forecasts, 66 pp.

——, M. Tiedtke and J-F. Geleyn, 1982: A short history of the PBL parameterization at the ECMWF. Proc., ECMWF Workshop on Planetary Boundary Layer Parameterization, 59–80.

Oort, A. H., and E. M. Rasmusson, 1971: Atmospheric circulation Statistics. NOAA Prof. paper, 5, U.S. Dept. of Commerce, Washington DC.

Panetta, R. L., I. Held and R. T. Pierrehumbert, 1988: External Rossby Waves in the 2-layer model. *J. Atmos. Sci.*, **44,** 2924–2933.

Pedlosky, J., 1982: *Geophysical Fluid Dynamics.* Springer-Verlag, 624 pp.

Pierrehumbert, R. T., 1986: Spatially amplifying modes of the Charney baroclinic instability problem. *J. Fluid Mech.*, **170,** 293–317.

Plumb, R. A., 1986: Three-dimensional propagation of transient quasigeostrophic eddies and its relationship with the eddy forcing of the time-mean flow. *J. Atmos. Sci.*, **43,** 1657–1670.

Sanders, F., 1987: Explosive cyclogenesis in the West-Central and North Atlantic ocean, 1981–1984. Part I: Composite structure and mean behavior. *Mon. Wea. Rev.*, **114,** 1781–1794.

Smagorinsky, J., 1963: General circulation experiments with the primitive equations. I: The basic experiment. *Mon. Wea. Rev.*, **91,** 99–164.

Williams, G. P., and J. B. Robinson, 1974: Generalized Eady waves with Ekman pumping. *J. Atmos. Sci.*, **34,** 1689–1695.

Young, R. E., and G. L. Villere, 1985: Nonlinear forcing of planetary scale waves by amplifying unstable baroclinic eddies generated in the troposphere. *J. Atmos. Sci.*, **42,** 1991–2006.